Current Sheet Applicators For Clinical Microwave Hyperthermia

M. K. Gopal, *Member, IEEE,* and T. C. Cetas, *Member, IEEE*

Abstract—**Current sheet applicators (CSAs) are light-weight, small size applicators intended to be operated in array configurations. Their radiative fields are induced by RF currents in a conducting sheet embedded a few millimeters below the dielectric covered aperture surface. In arrays, these elements can be used over breast lesions, for superficial head tumors, torso regions and other curved body sites where conformity to body curvatures is necessary. Our clinical prototypes are tuned to 434 MHz and have a bandwidth of almost 20 MHz, which accommodates the tuning and coupling changes due to site differences of the body, body movement and tissue heterogeneities. The relative insensitivity of these units to air bubbles in bolus and scar tissues are attractive clinical features. The inherent linear polarization allows easy visualization of the superposition of electric field vectors of each element of an array, as well as provides deeper penetration on curved surfaces due to the electric field vector addition in the medium. In the case of a large breast tumor, depth of heating of over 4 cm was achieved along the central axis of a 2×2 coherent array. Experimental evaluation of these elements, leading up to their clinical implementation, is described in detail along with the results of a clinical example.**

I. Introduction

HYPERTHERMIA combined with radiation has been shown to be much more effective in the destruction of cancer cells and tumors than radiation alone [1], [2]. The aim in hyperthermia is to raise the temperature of the tumor to greater than 42.5°C, at the same time, not to allow the temperature of the surrounding healthy tissues to rise to damaging levels (typically 44 to 45°C for periferal muscle). The success of the treatment lies in the capability of confining heat to the tumor volume. Superficial hyperthermia, induced with microwave applicators in general, is concerned with effective heating to depths of 2 to 3 cm. Typical frequencies are 434 MHz and 915 MHz for tumors with diameters of several centimeters [3]. In the USA, the ISM frequency for such use is 915 MHz, but 434 MHz is in common use in Europe. The radiating elements employed in commercial systems are still based on waveguide designs. These suffer from a list of drawbacks such as large size, low ratio of heating area compared to the physical aperture, sensitivity to tissue heterogeneities and inability to conform to body contours. The waves emanating from these apertures are nearly plane wave and the effective heating depth is controlled by the plane wave penetration depth [4], [5]. Lower frequencies are preferable for deeper penetration; but, either the waveguide size must be larger or more exotic, or high dielectric loading materials must be used. Modifications to waveguide radiators include partitioning with multiple feeds and incorporation of dielectric lenses [6], [7]. Even though these modifications alter the regular cosine square distribution of $|E|^2$ pattern, the size of the applicator still remains large.

Small microwave radiating elements used in an array have many advantages [8]–[10]. The array can be flexible so that it can conform to body contours. Individual elements can have independent power and phase control which will allow optimizations of the heating patterns and deposition of power at greater depths. Small radiating elements can be fabricated using microstrip designs [11]. Microstrip spirals have been used successfully as array elements in recent years [12]. These circularly polarized elements are operated incoherently in order to achieve wider superficial heating patterns. Microstrip patches also are suggested for use as elements in an array [13]. Another element suggested for this purpose is based on a current sheet or magnetic dipole distribution of the aperture [14]–[16]. The linear polarization of these elements allows vector field addition in the tumor volume thus enabling power deposition at deeper levels while simultaneously minimizing the power deposition in the overlaying fat and skin layers. Based on the current sheet principle, prototypes of current sheet applicators (CSAs) were designed, tested both singly and in arrays [9]. Theoretical predictions using an approximate analysis based on a Gaussian beam model were compared successfully with experimental results [17]. These early prototypes could not handle the power used in the clinical application and were not stable, so the elements were further engineered into frequency stable, low loss, high power units. Characterizations were carried out in the laboratory prior to implementation of these units at the University of Arizona Health Science Center, Tucson, AZ and Hammersmith Hospital, London. This paper presents the results of these laboratory tests along with a clinical example.

II. Evaluation of CSAs

The current sheet applicator is a distributed resonant circuit to which RF energy is coupled capacitively. A part of the resonant circuit which is not shielded acts as a radiating element to launch power into the body. Theoretical field computations and the advantages of magnetic dipole based applicators are published by Morita and Andersen [14]. Based on this principle, prototype applicators have been constructed

Manuscript received November 15, 1991; revised July 24, 1992. This work was supported in part by grants from the National Cancer Institute CA29653 and from the Arizona Disease Control Research Commission 82-2701.

The authors are with the Radiation Oncology Department, University of Arizona, Tucson, AZ 85724.

IEEE Log Number 9205444.

[9], [15], [16]. The present practical units are fixed tuned at 434 MHz but can be modified to operate between 350 and 1150 MHz without significant changes in physical dimensions or the tuned circuit configuration. The coupling between the radiating element and tissue is achieved by use of an appropriate water bolus. Coupling is affected also by the distance of the radiating element from the bolus. A moderate return loss is chosen (around -10 dB) so as to achieve a large bandwidth of approximately 20 MHz which is useful for overcoming the detuning effects caused by small drifting in the overall system, ambient temperature changes, element heating, local tissue heterogeneities and the load variations at different sites of the body.

The CSA has radiating face dimensions of 7.3 cm $\times$ 5.9 cm and it is 3.3 cm high. It weighs 340 gms. The radiating aperture is 6.1 cm $\times$ 5.2 cm. The electric field vector is polarized linearly parallel to the longer dimension. Depending upon the convective cooling by blood flow of the tissues being treated, the CSA may require anywhere from 10 to 80 watts input power for a successful clinical treatment. In the initial tests, a semi-solid phantom, which is a variation of the muscle phantom developed by Chou *et al.* [18] and modified by Nilsson [19] was used. It consisted of a 60% saline solution (2.5% NaCl and 97.5% H_2O), 22.5% sugar and 17.5% of a gelling agent TX-150 (Oil Center Research, 616 W. Pont des Mouton Rd, Lafayette, LA 70507). A 1 cm fat layer covered its top; its composition was 67% white flour, 30% oil and 3% saline (0.9% NaCl and 99.1% H_2O). The relative dielectric permittivity ϵ_r and conductivity σ of the phantom materials were measured by using a semi-automatic system based on a small monopole technique [21]. The ϵ_r and σ of muscle were 55 and 1.2 S/m, and for fat 7 and 0.05 S/m, respectively. The water bolus consisted of a 0.25 mm thick polyethylene bag, into which a fibrous material with an open porous structure (3M brand red colored industrial floor buffing pads), was inserted and sealed. The overall thickness of the bolus was about 1.5 cm.

The stability of the CSA at high power, as determined by the return loss curves, was first verified. The elements inside the unit carry substantial currents and therefore produce heat. Furthermore, the metallic body of the unit could heat from induced eddy currents. Two optical temperature sensors (Luxtron 3000) were attached to the current carrying elements inside the unit and another was attached to the body of the CSA, and 45 watts of power was applied to the unit. After approximately 30 minutes, the inside elements heated to nearly 75°C and stabilized. However the temperature of the body of the CSA did not begin to rise immediately upon power ON but rather began to rise approximately a minute after the power ON. This suggests that the body was heated by thermal conduction from other parts of the CSA rather than directly from eddy currents induced in the body. Nevertheless, the external temperature eventually rose to about 55°C; which was considered to be too hot for practical use by the technologists in the clinic. Radiating fins were added to the top and sides of the CSA. With these, the internal temperature stabilized at about 60°C. In clinical use, heat is dissipated by the water bolus and the elements feel comfortably warm to the touch, but not hot. In order to check the stability during long time operation, the unit was kept powered at 45 watts into a phantom material load for over an hour. The return loss curves at the beginning and end of the experiment were identical. The unit was then powered at 100 watts. The return loss comparison was checked again after 15 minutes, at which time the power was shut off because the phantom melted. Again no degradation was noticed. A visual examination, after dismantling the unit, also showed no signs of degradation of any components. These tests confirmed that the CSA can handle the power levels required in clinical treatments and function reliably.

Next the $|E|^2$ pattern measurement was carried out by scanning a dipole in a liquid phantom. The liquid phantom, with properties close to muscle, consisted of 35.6% ethyl alcohol, 63.2% water and 1.2% NaCl. The ϵ_r and σ were measured as before (57 and 1.2 S/m, respectively, at 434 MHz). This mixture filled a tank with a 0.075 mm thick polyethylene window. The window was covered with a 1 cm thick fat mixture and then the water bolus. The return loss characteristic for this configuration is shown in Fig. 1(a) as a function of frequency. It has a return loss and bandwidth of approximately 10 dB and 20 MHz respectively. A 4 mm long balanced dipole was used for mapping the electric field. A network analyzer (Hewlett Packard 8754A) was used to feed the signal to the CSA as well as to measure the probe output. The probe stepping and data collection were carried out by an automated system. Fig. 1(b) shows the $|E|^2$ contours, corresponding to the parallel and predominent polarization (E_{par}), over a plane 1 cm deep into the muscle medium and parallel to the face of the CSA. The contours are normalized with respect to the peak value in the same plane which is at the center of the frame. A total of four CSAs were made in our laboratory for clinical treatment purposes, and all four very well matched in their return loss characteristics and $|E|^2$ contour distributions.

The suitability of the CSAs for array configurations were presented earlier [9]. To reconfirm, these high power units were scanned as single units, a two element array and a four element (2×2) array. Both parallel and perpendicular planes (with respect to the face of the CSA) were scanned. In array configurations, the units were separated by 1 cm to reduce the mutual coupling [9]. Fig. 2 shows the $|E|^2$ contours over the parallel and perpendicular planes for a single CSA following a protocol established for maintaining quality assurance in hyperthermia trials [22]. In Fig. 2(a) the 25% contour at 1 cm into muscle covers 51% of the facial area of the CSA. The contours represent the 25% specific absorption rate (SAR) profile, as referred to the fat/muscle interface, for depths of 0.2, 1 and 2 cm from the interface. The maximum depth along the central axis, where the SAR drops to 25%, is also shown at the center. In a uniform media, like the muscle phantoms used in the experiments, the average power deposited at each point, by a plane wave, on a per unit volume basis is proportional to $|E|^2$, and so represents SAR. Fig. 2(b) shows 25% contour for the perpendicular central plane. These scans give an idea of the volume that is covered by the 25% contour. The use of 25% SAR for the definition of effective

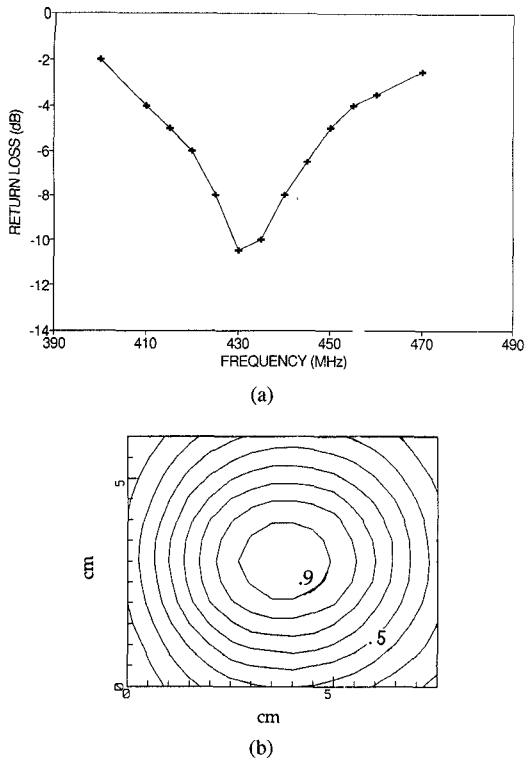

Fig. 1. (a) Frequency vs return loss characteristic for a CSA. It has a return loss of around -10 dB and a 3 dB bandwidth of approximately 20 MHz. (b) Normalized $|E|^2$ contours for a CSA at 1 cm depth into the muscle phantom.

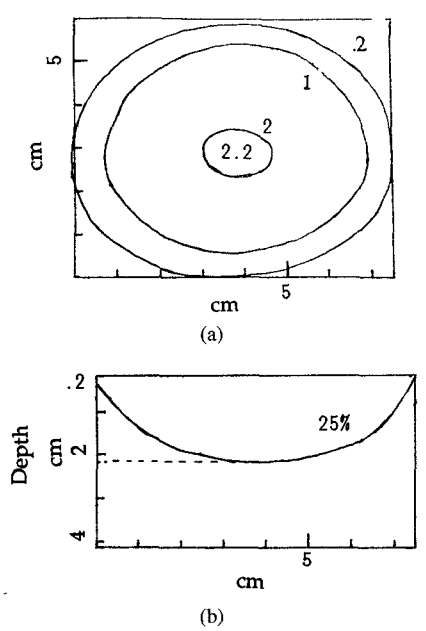

Fig. 2. (a) 25% $|E_{\mathrm{par}}|^2$ contours for a single CSA over planes 0.2, 1 and 2 cm into the muscle medium. The maximum depth of 25% controur (2.2 cm) is shown at the center of the frame. (b) 25% $|E_{\mathrm{par}}|^2$ contours over the perpendicular plane.

heating volume has been suggested as a means of standardizing descriptors of microwave applicators [22]. Coincidentally, the European definition of the same, which refers to the 50% SAR, normalized to the SAR value at 1 cm into muscle phantom [23] works out to about the same value. Figs. 3 and 4 show similar contours for 2 element arrays when the units are set up

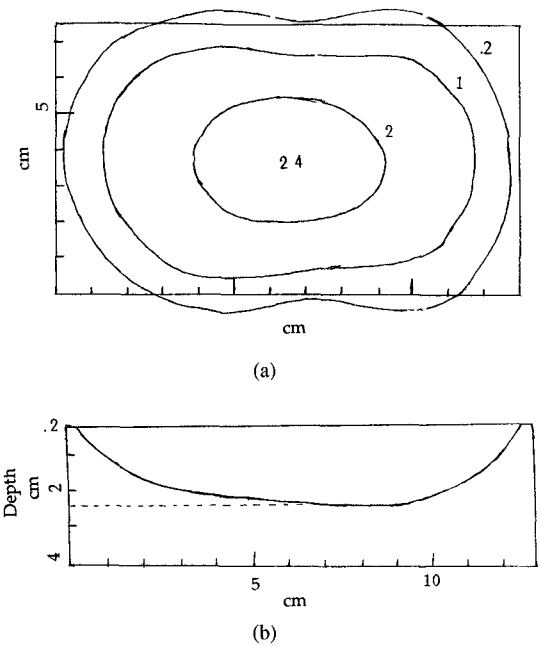

Fig. 3. (a) 25% $|E_{\mathrm{par}}|^2$ contours over planes 0.2, 1 and 2 cm into muscle for a 2 element CSA array with the longer edge side by side or with the electric field polarizations parallel to the common edge. (b) 25% $|E_{\mathrm{par}}|^2$ contour over the perpendicular plane.

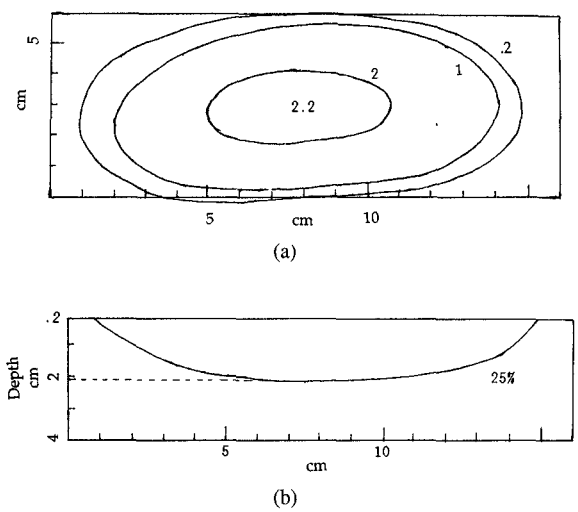

Fig. 4. (a) 25% $|E_{\mathrm{par}}|^2$ contours over planes 0.2, 1 and 2 cm into muscle for a 2 element CSA array with the shorter edge side by side or with the electric field polarizations perpendicular to the common edge. (b) 25% $|E_{\mathrm{par}}|^2$ contour over the perpendicular plane.

side by side with their electric field polarizations parallel and perpendicular to the common edges respectively. Fig. 5 shows the decay profile of $|E|^2$ in the muscle medium, starting at the fat/muscle boundary, along the axis of a single applicator. The value of $|E|^2$ at 1 cm depth is nearly half the value at the boundary. So the 25% contour area in Figs. 2 through 4 will approximately correspond to 50% contour area, or effective field size (EFS), if the $|E|^2$ readouts were normalized to the peak value at the 1 cm deep plane itself [23]. Similarly, the depth at which $|E|^2$ decays to half its peak value in the 1 cm plane, defined as effective heating depth (EHD), will be 1.2 cm for a single CSA.

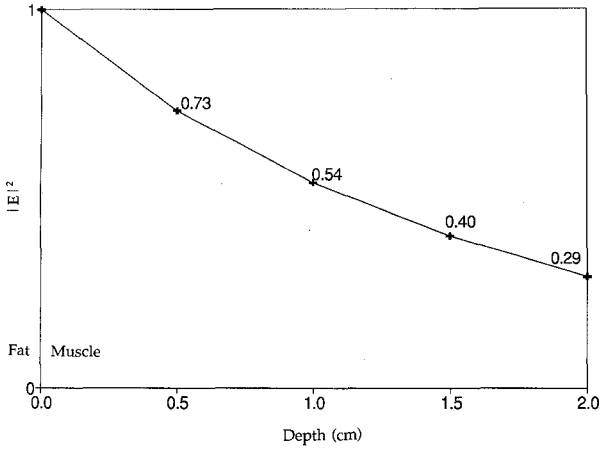

Fig. 5. The decay profile of $|E_{\mathrm{par}}|^2$ in the muscle medium starting at the fat/muscle interface.

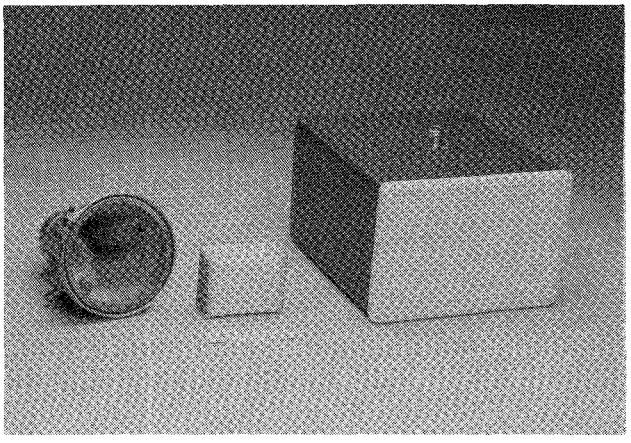

Fig. 6. Photographs of SMA, CSA and Lund applicators.

For comparison purposes, the measurements were also carried out on two other applicators which were used in our clinic for several years. The EFS for a SMA horn applicator (water filled horn) [24] and a Lund applicator [19] are 38% and 29% respectively. A comparison of the size differences between SMA, CSA and Lund applicators can be seen in Fig. 6. The EHD is a function of frequency and is nearly the same for all three applicators. However, if the aperture size is reduced much below the half wavelength, the penetration depth and EHD will reduce [10], [25], [26]. In general, since the 50% contours are contiguous in case of CSA arrays, it should be pointed out that when they are operated in arrays, the EFS can increase [9]. A comparison of the EFS for SMA, CSA (single and arrays) and Lund applicators are given in Table I. The lower value of EFS for the 2×2 array is due to the less than optimal geometric precision with which this particular array was assembled for the test.

Contrary to the waveguide applicators, the radiating current element in a CSA, operating with a magnetic dipole distribution, is a low impedance source and generates a magnetic or low impedance wave. Neglecting the small portion of the wavelength in the Teflon insulation, the near field interface $D^2/2\lambda$ is 2.4 cm deep (D is the largest aperture dimension

TABLE I
COMPARISON OF CHARACTERISTICS OF SMA, CSA AND LUND

Applicator	Maximum SAR W/kg/W_{in}	EFS %	Calorimetric Efficiency (%)
SMA horn	1.92	38	71
CSA (single)	1.85	51	77
CSA (2×1)	0.73	59	77
CSA (2×2)	0.75	46	81
Lund 12×18 cm	1.08	29	55

and λ is the wavelength in the bolus medium). So the 1.5 cm thick water bolus sets the skin within the near field region and the wave, at this point, has a slight predominance of H-field over E-field [27]. The permeability μ_r of the tissue is the same as that of water (and indeed that of free space). However, the ϵ_r of scar tissues, skin folds, fat and other tissues present variations which lead to tuning and coupling differences for waveguide applicators. In contrast, the somewhat near field nature of the wave launched from the CSA does not cause appreciable tuning or coupling differences. This is seen in the laboratory where air bubbles of a few millimeter diameter were simulated by 2 to 4 mm sized styrofoam chips spread over the fat layer, and later inside of the bolus as well. These simulated bubbles caused a maximum variation in return loss of 0.8 dB at 434 MHz (with an unperturbed return loss of 10 dB in Fig. 1(a)). In the clinic, air bubbles of 1 cm diameter are not noticeable in the performance characteristics as inferred from the reflected power variations. A comparison of waveguide, resonant patch and inductive applicators by Johnson *et al.* [28] also shows the relative insensitivity to load variations of inductive (or current sheet) applicators over the other two.

The normal component of the electric field cannot be ignored since the continuity relation of electric flux density causes the normal component in the fat layer to be much higher than in muscle. The ϵ_r for muscle and fat are approximately 55 and 7 respectively, and so the normal component in fat, near the interface of the two media, will be higher by the ratio of these, or about 8 times. Strong normal components can lead to hot spots in the overlying fatty tissues. The normal component was measured by positioning the dipole of the scanning probe along the axis of the applicator. The network analyzer and an automatic scanning system was used to map the fields as before, but the measurement was done very close to the muscle/fat boundary (2 mm into the muscle medium, the closest the probe could be positioned). Fig. 7 gives the contours of $|E_{\mathrm{nor}}|^2$ normalized to the peak value of the normal component in the same plane. The asymmetry of the normal component contours reflects the fact that the CSA circuitry is unbalanced. The outer conductor of the feed cable is grounded to the case of the CSA. In Fig. 8, the normal component for a mid-line section is shown along with the corresponding parallel component. The ratio of the peak parallel component to the peak normal component of $|E|^2$ is also given. The same ratio in the fat layer is found by using the electric flux continuity relation. This gives a normal component in fat layer which is nearly twice the parallel component.

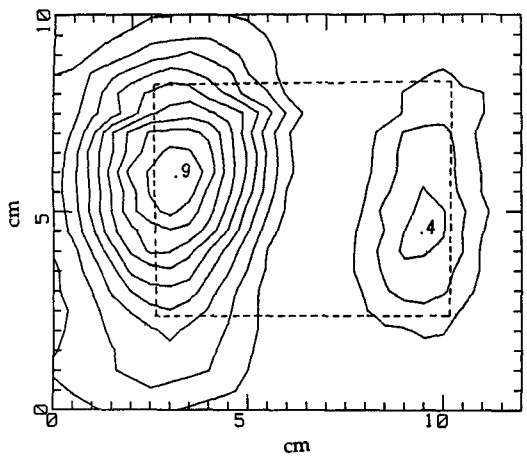

Fig. 7. $|E_{\mathrm{nor}}|^2$ contours for a single CSA in muscle medium close to the fat/muscle boundary (0.2 cm). Curves are normalized to the peak value in the same plane. Notice the asymmetry of the contours on either side, which is due to the unbalanced feed arrangement inside the CSA. The dashed frame shows the CSA boundaries.

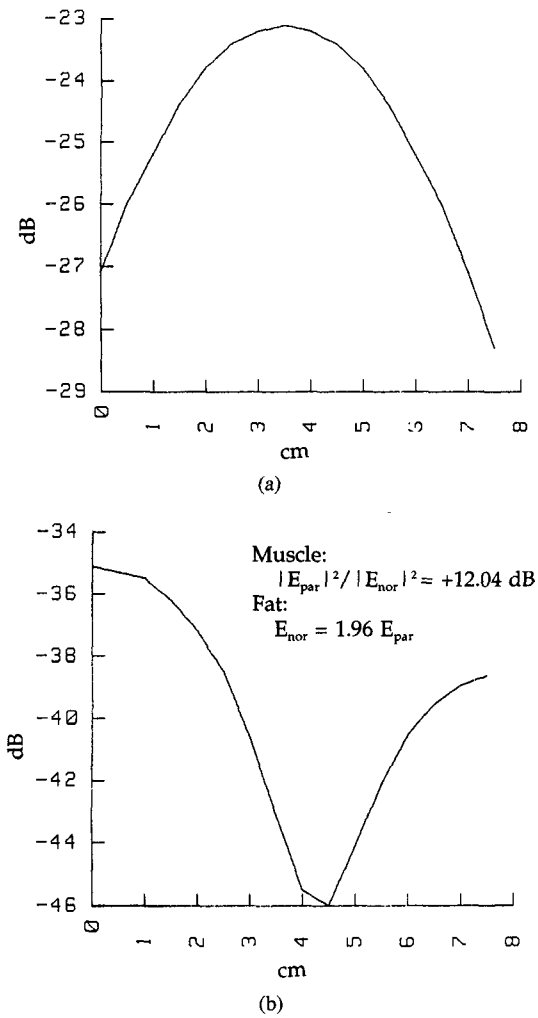

Fig. 8. (a) Plot of $|E_{\mathrm{par}}|^2$ along the mid-line of Fig. 1(b). (b) Plot of $|E_{\mathrm{nor}}|^2$ along the mid-line of Fig. 7. The relative strengths of parallel and normal components in muscle (close to the fat/muscle interface) and the fat layer are also shown.

Similar measurements on an SMA applicator [24] gave a normal component 2.1 times the parallel component. The normal component of SMA applicator is strong at one edge of the horn near the coaxial feed. For CSAs, an asymmetry in the normal component arises from the unbalanced feed arrangements inside the unit. Changing to a balanced feed arrangement reduced the normal component down to 1.7 times the parallel component. We are not aware of published data on the normal components of commercial applicators at 434 MHz; but the normal component to parallel component ratio of certain 915 MHz microstrip antenna arrays seems to exceed that of waveguide arrays to a depth of over 2 cm [3].

A calorimetric efficiency test [29] was carried out to evaluate the effectiveness of CSA in comparison to the other types of radiating elements used in our clinic. Here a 0.9% saline solution replaced the muscle medium. No fat or bolus was used. The coupling to the calorimeter was very good resulting in a return loss of -14 dB. The applicator was kept in contact with a 0.075 mm thick polyethelene membrane covering the saline solution. The power absorbed by the saline solution was calculated from the temperature rise in the saline medium. The forward and reflected powers were measured, at the input connector of the CSA, with a Hewlett-Packard Model 436A power meter and the difference was taken as the true input power. The ratio of the absorbed power to the net input power gives the calorimetric efficiency for the CSA as 77%.

The specific absorption rate (SAR) along the central axis of the CSA (both single and arrays) at 1 cm into the muscle medium was measured using the semi-solid muscle phantom with the fat layer and bolus on top of it. Forward power of 100 watts was fed to the CSA for 1 minute, and the temperature rise at the desired point in the muscle medium was measured using an optical thermometry probe (Luxtron 3000). In the absence of diffusion, the absorbed power is given by $c\Delta T/\Delta t$ where c is the specific heat of the phantom muscle medium in joules/kg/°C (taken as 0.83 times that of water), ΔT is the temperature rise and Δt is the time over which the power was ON. This value was divided by the input power to get an SAR of the element in watts/kg/watts-input. This is a number that can be used for quantitative comparison of the effectiveness of different applicators. The SARs calculated from the above for SMA, CSA and Lund applicators are given in Table I. All applicators were operated at 434 MHz. The low values for 2×1 and 2×2 CSA arrays is a result of the flatter field profiles compared to the peak value for a single applicator, horn or otherwise.

Return loss readings were taken on the chestwall and abdomen of 5 volunteers to assess the variation in the coupling at different sites. On the chestwall, the readings were taken with the electric field polarization both parallel and perpendicular to the ribs. As a reference, the same reading was taken on a standard muscle and fat phantom. The return loss at 434 MHz on the phantom was -9.2 dB. On the abdomen, this parameter varied from -6.5 to -7.5. On the chestwall, it varied from -7 to -8.3 and -9.5 to -10.5 respectively, when the electric field was parallel and perpendicular to the ribs. Note the higher coupling in the latter case. The muscle between ribs are conductive with σ of 1.2 S/m whereas the bone, which is similar to fat, is a poor conductor with a σ of 0.05 S/m. The relatively highly conducting narrow muscle

TABLE II
SAR VALUES COMPUTED FROM THE BREAST PHANTOM EXPERIMENT OF FIG. 9. THE PERCENTAGE OF THE AVERAGED SARS AT THE BOTTOM AND CENTRAL EDGE OF THE TUMOR WITH RESPECT TO THE CENTRAL AXIS ARE SHOWN IN THE LAST COLUMN

Sensor	SAR	% (average of sensors)
1	3.82	
2	5.16	
3	6.25	
4	5.19	100 (1–4)
5	0.86	
6	1.84	26 (5–6)
7	2.61	
8	3.41	
9	2.61	
10	3.67	60 (7-10)

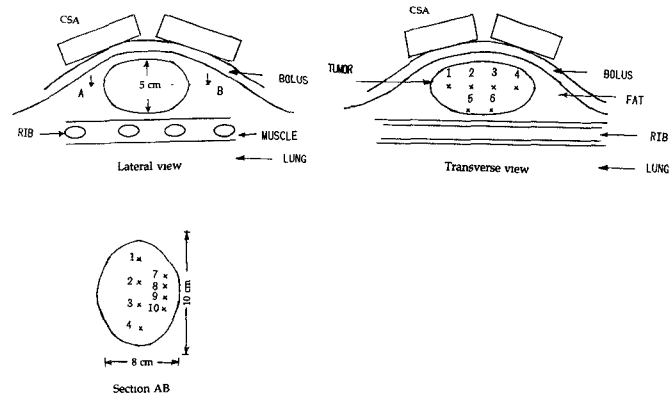

Fig. 9. Sketch of the phantom simulation of the breast tumor. The numbers 1 to 10 represent the temperature sensor locations.

regions between the bones are analogous to the wires in a wire grid polarizer. Hence the electric field can penetrate deeper if the polarization is perpendicular to the ribs.

III. MODEL OF A CLINICAL CASE

From December, 1989, until the time of writing this paper, at the University of Arizona, 19 patients underwent microwave hyperthermia treatments using the CSAs, many with multiple treatments. Of these, 7 were breast or chestwall sites and the remainder were neck, superclavicular, leg, head, shoulder, abdomen, face, leg and groin. One case, where the coherent phasing of a 2×2 array led to a successful clinical heating of deeper layers, is substantiated below.

The tumor, located in an in-tact breast, approximated an ellipsoid with axes of 10 cm (transverse) and 8 cm (lateral), with a depth of 5 cm (anterior-posterior). To heat this entire volume, four CSAs in a 2×2 array format were used. To construct a replica, approximate dimensions of the thickness of the muscle, rib and fat were taken from a CT scan of the patient. Ribs have approximately the same electrical characteristics as fat. Lung phantom material is similar to muscle phantom material but with $\epsilon_r = 35$ and $\sigma = 0.3$ S/m. It was inserted under the overlying fat and the muscle-rib layer. The individual CSAs were tilted through an angle of approximately 20° in order to conform to the curvature of the simulated breast. The bolus bag was modified to permit conformance of the bag to the 'breast phantom' surface. The set up is illustrated in Fig. 9. Ten fiber optic thermometry probes (Luxtron 3000) were laid out, as shown in the figure represented by numbers 1–10, in order to measure the SAR and temperature distribution over the central axis of the tumor, tumor boundary and bottom of the tumor. Thirty watts forward power was fed to each applicator for 2 minutes and the temperatures were recorded. From the initial slope of the temperature vs time curve, the SAR values were calculated. If averages of these SARs are taken and compared, the tumor boundaries in its central plane and bottom have average SARs of 60% and 26% respectively compared to the average SARs along the major axis, which is taken as 100%.

In the actual treatment the temperature sensor positions inside the tumor were located from a CT scan of the patient. The SAR values, computed from cdT/dt, at the base of the tumor and the core were nearly the same. This result is better than the phantom simulation. This indicates that the phantom model did not exactly correspond to the clinical case. The heat loss through blood flow and the focussing of the energy at the bottom of the tumor may be the cause for this difference. Nevertheless, the model was good enough to establish feasibility prior to treatment and the treatment was successful in terms of the measured temperatures in the tumor (mean of 42.3°C averaged over 18 measurement locations with a range of 41.2 to 44°C). Two measured locations outside the tumor were at 43.3°C and 42.9°C. All other measured points outside the tumor were below 41.5°C. The tumor reduced to $4 \times 4 \times 3$ cm, three months after the treatment and has remained stable in size for nine months to the date of writing this paper.

IV. CONCLUSION

CSAs are small, stable and robust applicators capable of withstanding the high power levels used in the clinic without degradation, and are suitable for use in clinical hyperthermia. Our present model weighs 340 gms, is 7.3 cm long, 5.9 cm wide and 3.3 cm high. They can be used as single stand alone elements or as elements in a large array. As single elements, the small size allows their use in treating neck nodes and other similarly constricted areas. In arrays, these elements can be used on breast lesions, on the head for superficial brain tumors, for torso regions and for other curved sites of the body where conformity to the body is necessary. The linear polarization of these units allows easy visualization of the electric field vectors which helps in the proper orientation of the applicators. On curved sites the linear polarization provides deeper penetration due to field vector addition [20], [30].

ACKNOWLEDGMENT

Discussions with Dr. J. W. Hand have been very helpful. The patient was under the clinical care of Dr. B. Stea. Anne Fletcher and Suzanne Dyet carried out the clinical treatments and assited in the reduction of the patient data.

REFERENCES

[1] G. M. Hahn, "Hyperthermia for the engineer: A short biological primer," *IEEE Trans. Biomed. Eng.*, vol. BME-31, pp. 3–8, Jan. 1984.

[2] J. Overgaard, "The rationale for clinical trials in hyperthermia," in *An Introduction to the Practical Aspects of Clinical Hyperthermia,* S. B. Field and J. W. Hand, Eds., London: Taylor & Francis, 1990, pp. 213–241.

[3] R. L. Magin and A. F. Peterson, "Noninvasive microwave phased arrays for local hyperthermia: A review," *Int. J. Hyperthermia,* vol. 5, no. 4, pp. 429–450, 1989.

[4] J. W. Hand and A. J. Hind, "A review of microwave and rf applicators for localized hyperthermia," in *Physical Techniques in Clinical Hyperthermia*, J. W. Hand and J. R. James, Eds., Letchworth, UK: Research Studies Press, 1986, pp. 98–148.

[5] J. W. Hand and R. H. Johnson, "Field penetration from electromagnetic applicators for localized hyperthermia," *Recent Results in Cancer Research,* vol. 101, pp. 7–17, 1986.

[6] G. H. Nussbaum and L. B. Leybovich, "Externally induced EM hyperthermia: microwave techniques," in *Proc. 8th annual conf., IEEE/Biol. Med. Eng.*, Fort Worth, TX, Nov. 1986.

[7] Y. Nikawa, M. Kikuchi and T. Matsuda, "Heating system with a lens applicator for 430 MHz microwave hyperthermia," *Int. J. Hyperthermia,* vol. 6, no. 3, pp. 671–684, 1990.

[8] J. W. Hand, J. L. Cheetham, and A. J. Hind, "Absorbed power distributions from coherent microwave arrays for localized hyperthermia," *IEEE Trans. Microwave Theory Tech.,* vol. MTT-34, pp. 484–489, 1986.

[9] M. K. Gopal, J. W. Hand, M. L. D. Lumori, S. Alkhairi, K. D. Paulsen, and T. C. Cetas, "Current sheet applicator arrays for superficial hyperthermia of chestwall lesions," *Int. J. Hyperthermia,* vol. 8, no. 2, pp. 227–240, 1992.

[10] R. H. Johnson, G. Andrasic, D. L. Smith, and J. R. James, "Field penetration of arrays of compact applicators in localized hyperthermia," *Int. J. Hyperthermia,* vol. 1, no. 4, pp. 321–336, 1985.

[11] I. J. Bahl, S. S. Stuchly, and M. A. Stuchly, "A new microstrip radiator for medical applications," *IEEE Trans. Microwave Theory Tech.,* vol.MTT-28, pp. 1464–1468, 1980.

[12] T. V. Samulski, P. Fessenden, E. R. Lee, D. S. Kapp, E. Tanabe, and A. McEuen, "Spiral microstrip hyperthermia applicators: technical design and clinical performance," *Int. J. Radiation Oncology Biol. Phys.,* vol. 18, pp. 233–242, 1990.

[13] R. H. Johnson, J. R. James, J. W. Hand, J. W. Hopewell, P. R. C. Dunlop, and R. J. Dickinson, "New low-profile applicators for local heating of tissues," *IEEE Trans. Biomed. Eng.,* vol. BME-31, no. 1, pp. 28–37, Jan. 1984.

[14] N. Morita and J. B. Andersen, "Near field absorption in a circular cylider from electric and magnetic line sources," *Bioelectromagnetics,* vol. 3, pp. 253–274, 1982.

[15] J. B. Andersen, A. Baun, K. Harmark, L. Heinzl, P. Raskmark and J. Overgaard, "A hyperthermia system using a new type of inductive applicator," *IEEE Trans. Biomed. Eng.,* vol. BME-31, no. 1, pp. 21–27, 1984.

[16] R. H. Johnson, A. W. Preece, J. W. Hand and J. R. James, "A new type of lightweight low-frequency electromagnetic hyperthermia applicator," *IEEE Trans. Microwave Theory Tech.,* vol. MTT-35, pp. 1317–1321, 1987.

[17] M. L. D. Lumori, J. W. Hand, M. K. Gopal and T. C. Cetas, "Use of Gaussian beam model in predicting SAR distributions from current sheet applicators," *Phys. Med. Biol.,* vol. 35, no. 3, pp. 387–397, 1990.

[18] C. K. Chou, G. W. Chen, A. W. Guy, and K. H. Kuk, "Formulas for preparing phantom muscle tissue at various radiofrequencies," *Bioelectromagnetics,* vol. 5, pp. 435–441, 1984.

[19] P. Nilsson, "Physics and technique of microwave-induced hyperthermia in the treatment of malignant tumors," Ph.D. thesis, University of Lund, pp. 33–36, 1984.

[20] P. Nilsson, T. Larsson, and B. Persson, "Absorbed power distributions from two tilted waveguide applicators," *Int. J. Hyperthermia,* vol. 1, no. 1, pp. 29–43, 1985.

[21] E. C. Burdette, F. L. Cain, and J. Seals, "In vivo probe measurement technique for determining dielectric properties at VHF through microwave frequencies," *IEEE Trans. Microwave Theory Tech.,* vol. MTT-28, no. 4, pp. 414–427, 1980.

[22] M. W. Dewhirst, T. L. Phillips, T. V. Samulski *et al.,* "RTOG quality assurance guidelines for clinical trials using hyperthermia," *Int. J. Radiat. Oncol. Biol. Phys.,* vol. 18, pp. 1249–1259, 1990.

[23] J. W. Hand, J. J. W. Lagendijk, J. B. Andersen, and J. C. Bolomey, "Quality assurance guidelines for E.S.H.O. protocols," *Int. J. Hyperthermia,* vol. 5, no. 4, pp. 421–428, 1989.

[24] G. A. Lovisolo, M. Adami, G. Arcangeli, A. Borrani, G. Calamai, A. Cividalli, and F. Mauro, "A multifrequency water-filled waveguide applicator: Thermal dosimetry in vivo," *IEEE Trans. Microwave Theory Tech.,* vol. MTT-32, no. 8, pp. 893–896, Aug. 1984.

[25] J. B. Andersen, "Theoretical limitations on radiation into muscle tissue," *Int. J. Hyperthermia,* vol. 1, pp. 45–56, 1985.

[26] E. Cheever, J. B. Leonard, and K. R. Foster, "Depth of penetration of fields from rectangular apertures into lossy media," *IEEE Trans. Microwave Theory Tech.,* vol. MTT-35, pp. 865–867, 1987.

[27] D. R. J. White, *A Handbook Series on electromagnetic Interference and Compatibility,* vol. 2, Don White Consultants, Inc., Gainesville, VA, pp. 2.7–2.14, 1980.

[28] R. H. Johnson, A. W. Preece, and J. L. Green, "Theoretical and experimental comparison of three types of electromagnetic hypertermia applicators," *Phys. Med. Biol.,* vol. 35, no. 6, pp. 761–779, 1990.

[29] D. Anhalt and K. Hynynen, "The efficiency of clinical microwave applicators measured by a calorimetric method," *Med. Phys.,* vol. 15, no. 6, pp. 919–921, 1988.

[30] J. W. Hand, K. D. Paulsen, M. L. D. Lumori, M. K. Gopal, T. C. Cetas, and S. Alkhairi, "Microwave array applicators for superficial hyperthermia," in *Hyperthermic Oncology,* T. Sugahara and M. Saito, Eds., London: Taylor & Francis, 1989, pp. 827–828.

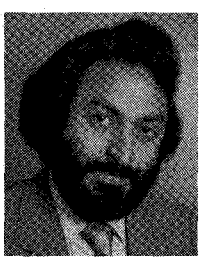

Mohan Krishnan Gopal (M'91) received the B.Sc. Engineering degree in electrical engineering in 1970 from the University of Kerala, India, and the M. Tech (master's) degree in 1973 from I.I.T., Madras, India.

From 1974 to 1981 he was employed as a satellite system integration and testing engineer at the Indian Space Research Organization, Bangalore, India. In 1983 he earned another master's degree in electrical engineering from the University of New Hampshire, Durham and later joined the University of Arizona. At both universities he was employed as Research Assistant in the department of Physics and/or Astronomy. Since 1987 he has been with the Department of Radiation Oncology, University of Arizona, Tucson, where he is actively involved in the design, development, testing and implementation of RF devices and systems for the hyperthermic treatment of cancer.

Thomas C. Cetas (M'85) received the Ph.D. degree in physics from Iowa State University, Ames, in 1970.

From 1970 to 1973 he was with the National Measurement Laboratory, Sydney, Australia, and from 1973 to 1975 he was with the National Bureau of Radiological Health, FDA. Since 1975 he has been with the Department of Radiation Oncology, University of Arizona College of Medicine, Tucson, where his research has been on the physical aspects of hyperthermia for cancer therapy. He holds joint appointments in Electrical and Computer Engineering and in Aerospace and Mechanical Engineering.